Synergism of Dimethoxybenzosemiquinone Free Radicals and CD4+ T-Lymphocytes to Suppress Ehrlich Ascites Tumor (44209)

CLINTON D. MORGAN,*[,1] STANLEY S. LEFKOWITZ,* AND JOHANNES EVERSE†

Department of Microbiology and Immunology and Department of Cell Biology and Biochemistry,† Texas Tech University Health Sciences Center, Lubbock, Texas 79430, USA*

Abstract. **Numerous natural and synthetic quinone compounds possess significant antitumor properties. Various mechanisms have been proposed to account for these properties, including scission and degradation of tumor cell DNA, intracellular "redox cycling" to cogenerate semiquinone free radicals and reactive oxygen intermediates, and the interaction of semiquinone radicals with tumor cell surface flavoenzymes. However, no evidence has been presented to explain adequately the preferential attack on tumor cells by semiquinone radicals, as opposed to normal cells. To address this question, a synergistic interaction was examined. A therapy consisting of a mixture of L-ascorbate and 2,6-dimethoxy-p-benzoquinone, was used for *in vivo* evaluation. BALB/c mice were depleted of functional T-lymphocytes by xenogeneic monoclonal antibody pretreatment, challenged with Ehrlich ascites tumor, and administered the semiquinone radical-generating therapy. Mice depleted of CD4+ T-lymphocytes responded with rapidly fatal tumor progression, with significantly decreased mean survival times over controls, whereas less severe responses were observed in mice devoid of CD8+ T-lymphocytes. Mice depleted of both T-lymphocyte subpopulations responded with uninhibited tumor growth and rapid mortalities. When tumor challenge occurred after therapy, tumor growth was significantly delayed in mice enriched for CD4+ T-lymphocytes, with demonstrable increases in mean survival time over controls. This reagent combination had no significant effect on T-lymphocyte profiles in secondary lymphoid organs. These data suggest a synergistic phenomenon of semiquinone radical-induced cytostasis coupled with T-lymphocyte helper activity for optimal tumor suppression.** [P.S.E.B.M. 1998, Vol 217]

Quinones occur naturally as benzoquinones, napthquinones, and anthraquinones and represent the largest class of quinoid compounds (1, 2). Natural and synthetic p-benzoquinones have appreciable antitumor activities, with the most useful containing reactive or heterocyclic side groups around aromatic base structures. Anthraquinones also possess significant antitumor activities (2, 3). These compounds undergo facile reduction and oxidation reactions; a one-electron reduction of a quinone generates a semiquinone-free radical, whereas a two-electron reduction creates a hydroquinone moiety (2). A phenomenon of "bioreductive activation," by virtue of repetitive reduction-oxidation reactions (redox cycling) has been a prominent hypothetical mechanism-of-action of the clinically significant benzoquinone and anthracycline antitumor agents (3–6).

The physicochemical properties and apparent *in vivo* antitumor activities of several structurally simple benzoquinone compounds were initially evaluated by Pethig *et al.* (7–9) within the context of free radical formation and subsequent reactivity. These studies revealed that mixtures of L-ascorbate and certain benzoquinone compounds exerted a

[1] To whom requests for reprints should be addressed at Division of Immunology, Department of Pathology, Scott & White Memorial Hospital and Clinic, 2401 South 31st Street, Temple, TX 76508, USA.

This work was supported by an institutional research grant from Texas Tech University Health Sciences Center and by a grant from the American Institute for Cancer Research.

Received May 2, 1997 [P.S.E.B.M. 1998, Vol 217]
Accepted July 11, 1997

0037-9727/98/2171-000$10.50/0

profound antitumor effect in mice challenged with Ehrlich ascites tumor. Ascorbate was employed as a non-toxic reducing agent to generate semiquinone free radicals from the parent benzoquinones. The respective abilities of these compounds to generate radicals were evaluated with *in vitro* and *in vivo* experimental approaches. Neither the ascorbate nor the benzoquinone compounds by themselves demonstrated significant levels of tumor inhibition, since the progression of the tumor was not retarded by the administration of the individual reagents. These results suggested that the observed antitumor effect of the combination therapy(ies) was a direct consequence of the formation of semiquinone free radicals, the reaction products generated in mixtures of ascorbate and these benzoquinone compounds.

The primary objective of the present study was to determine whether the semiquinone radical generated by the combination of L-ascorbate and 2,6-dimethoxy-p-benzoquinone, hereafter referred to as ASC/DMBQ therapy, interacted with specific immune response cells to suppress tumor growth. The reported cytostatic effect of the treatment protocol was considered relevant, and additional *in vivo* evaluations with specific immunodeficient animal models were necessary to establish a possible link with the cellular immune system.

Materials and Methods

Experimental Animals. BALB/c mice, age and sex matched, were employed in these studies and were obtained from Sasco, Inc. (Omaha, NE). The care and use of these animals conformed to the policies and regulations of the Institutional Animal Care and Use Committee of Texas Tech University Health Sciences Center.

Tumor Model. The wild-type Ehrlich ascites tumor was generously provided by Dr. L. M. Slater, University of California at Irvine, and was used throughout these studies. This tumor has been employed in numerous studies of tumor immunology and chemotherapy because of ease of transmissibility and growth characteristics (10–13). The tumor was maintained *in vivo* by weekly intraperitoneal (ip) injections of 200 μl tumor ascites into naive recipient BALB/c mice.

Hybridomas and Monoclonal Antibodies. Hybridomas GK1.5 (rat anti-mouse L3T4a/CD4+) and 2.43 (rat anti-mouse Lyt 2.2/CD8+) were obtained from the American Type Culture Collection (Gaithersburg, MD). The method of Sprent and Schaffer (14) was employed to induce large-scale *in vivo* production of ascites with each hybridoma. Briefly, mice were first primed by ip injection of 0.5 ml pristane (Sigma Chemical Co., St. Louis, MO). After 7–10 days, rabbit polyclonal anti-mouse lymphocyte serum (Accurate Chemical and Scientific Corp., Westbury, NY) was administered by ip injection of 100 μl per mouse. Twenty-four hours later these mice were subjected to sublethal whole body irradiation (500 rads of whole body exposure; 0.47-minute exposure for each group of 10 mice in a J.L. Shepherd Blood Irradiator, Model 143, equipped with a ^{137}Cesium source). Viable hybridoma cells (3–5 × 10^6 cells/100 μl) were injected ip 24 hr following irradiation.

After 7–14 days, hybridoma ascites were harvested from these mice by ip tap. Crude ascites were pooled and centrifuged to remove the hybridoma cells; cell-free ascitic fluids were then delipidated with 1,1,2-trichlorofluoroethane and stored at −70°C. The methods of Hornbeck (15) and Morrow *et al.* (16) were adapted for the detection and titration of the desired mAb in the clarified ascitic fluids by enzyme-linked immunosorbent assay. End-point titrations of these fluids were typically > 100,000 by reciprocal dilution (data not shown).

In Vivo Depletion of Differentiated T-Lymphocytes. The depletion procedure was adapted from the method of Husman and Bevan (17) and was consistent with similar reported manipulations (18–20). Briefly, clarified hybridoma ascitic fluids (200 μl) were administered to mice by ip injection; mice to be depleted of CD4+ T-lymphocytes received clarified GK1.5 ascites, and mice to be depleted of CD8+ T-lymphocytes received clarified 2.43 ascites. Mice to be depleted of both subpopulations received concurrent injections of both ascitic fluids. Control mice received ip injections of phosphate buffered saline (PBS, pH 7.4), also at 200 μl each.

Isolation and Labelling of Lymphocytes for Flow Cytometric Analysis. On a predetermined time schedule, mice were randomly selected from each group and euthanized by cervical dislocation. Cell suspensions were prepared from secondary lymphoid organs harvested from the mice and adjusted to 2 × 10^6 viable cells/ml in PBS supplemented with 1% bovine serum albumin (BSA) and 0.02% sodium azide (PBS/1% BSA/0.02% NaN_3). The standard labelling technique was used to stain these cells for indirect immunofluorescence analysis by flow cytometry. Clarified hybridoma ascitic fluids containing high titers of GK1.5 and 2.43 mAb and mAb 30-H12 (rat anti-mouse Thy 1.2, pan T marker; Boehringer-Mannheim Biochemicals, Indianapolis, IN) served as primary antibodies, and FITC-conjugated goat anti-rat IgG (whole molecule; Cappel/Organon Teknika Corp., West Chester, PA) served as the secondary detection reagent. Propidium iodide was added to all cell suspensions (10 μl of 50 μg/ml stock solution in PBS) as an indicator of cell viability and to allow the exclusion of dead cells in demonstrating the status of cells exhibiting specific surface phenotypes (21). Final cell suspensions were maintained on ice in the dark until analysis. A FACStar Plus flow cytometer (Becton-Dickinson Immunocytometry Systems, Mountain View, CA) was used to acquire data from 10^4 viable cells from each labelled suspension.

Preparation of Treatment Reagents. The quinone compound 2,6-dimethoxy-p-benzoquinone (DMBQ), was generously provided by Dr. G. Fodor, West Virginia University, Morgantown, WV. L-ascorbate (ASC) was obtained from Sigma Chemical Co. DMBQ was prepared at a concentration of 3 mM in PBS, and ASC was prepared at a

concentration of 750 mM, also in PBS. Both solutions were sterilized by passage through 0.22 μm Millex GV syringe filters (Millipore Corp.) into sterile disposable syringes. Fresh solutions were prepared daily for the standard treatment protocol.

Tumor Challenge and Administration of ASC/DMBQ Therapy to Mice Deficient in T-Lymphocyte Subpopulations. Mice were challenged 72 hr after T-lymphocyte depletion by ip injection of 100 μl of Ehrlich ascites tumor cell suspension (10^5 viable tumor cells in PBS supplemented with 2 mg/ml dextrose). The administration of ASC/DMBQ therapy or PBS was initiated 24 hr following tumor implantation. The treatment regimens consisted of two ip injections of the semiquinone radical-generating reagents (0.25 ml of each solution co-mingled in a dual syringe manifold) for 7 consecutive days, with the daily injections administered 10–12 hr apart. Control mice received similar volumes of PBS on the same schedule. The calculated dosages of ASC and DMBQ per injection were 1.86 mg/g and 0.006 mg/g body weight, respectively, with the initial mean body weight of each mouse at 20 g. All experimental and control mice were examined daily to document the onset of solid tumor formation, tumor ascites accumulation, and eventual survival times.

Alternately, mice were depleted of specific T-lymphocytes, as described previously, and were administered either ASC/DMBQ or PBS for the standard 7-day treatment protocol. Tumor challenge was withheld until 24 hr past the conclusion of ASC/DMBQ or PBS therapies, with the eventual tumor load at the same viable cell concentration as used previously. The results of the studies described herein were from single experiments encompassing large numbers of experimental and control mice for statistical inference.

Effect of ASC/DMBQ Therapy on T-Lymphocyte Subpopulations in Tumor-Free Mice. Immunocompetent, tumor-free mice were administered the standard 7-day ASC/DMBQ ip therapy to assess possible adverse consequences on T-lymphocyte profiles. Control mice received PBS ip at the same injection volume and frequency. Control and treated mice were euthanized at specified intervals, and spleens and selected lymph nodes (bilateral brachial, superficial cervical, superficial inguinal, and mesenteric nodes) were collected. Cell suspensions were prepared from these organs and stained for indirect immunofluorescence analysis, as previously described.

Statistical Analysis of Experimental Results. The arithmetic average (mean), the standard deviation (SD), and the standard error of the mean (SEM) were calculated as descriptive statistics for each set of replicative data. Ranges and median values for experimental and control responses were also calculated. Where appropriate, comparisons between the experimental means were made with *t* tests for paired and unpaired observations. Significant differences were denoted at $p \leq 0.05$.

Results

Kinetics of *In Vivo* Depletion and Repopulation of T-Lymphocytes. The kinetics of depletion/repopulation of T-lymphocytes are shown in Table I. Single ip injections of clarified GK1.5 and 2.43 ascitic fluids resulted in > 95% depletion of the respective T-lymphocyte subpopulations for at least 15 days. Gradual repopulation of T-lymphocytes expressing the CD4+ and CD8+ phenotypes was observed thereafter. However, a reduction of > 90% was clearly evident for almost 30 days. The rate of CD8+ repopulation appeared to exceed the general rate of CD4+ repopulation, but this may have simply reflected divergent concentrations of cells in murine lymph nodes.

Manipulation of T-lymphocyte profiles with mAb significantly altered CD4:CD8 ratios. The PBS control mice exhibited ratios consistently near the low end of the normal range of 2.0–2.5 (data not shown). GK1.5-treated mice exhibited ratios near zero in the majority of the assays whereas 2.43-treated mice exhibited ratios that far exceeded control ratios. Repopulation of CD4+ and CD8+ T-lymphocytes over the designated time span was incomplete, yet the trend to restore the normal CD4:CD8 ratios was clearly demonstrated.

Solid Mass Development in ASC/DMBQ-Treated Mice Deficient in T-Lymphocyte Subpopulations. Palpable solid tumor masses at or near the sites of tumor implantation were detected by daily examination of the mice. The relative time, in days, for solid mass development between the various groups of mice is shown in Figure 1. All control mice quickly developed detectable masses, regardless of cellular deficiency or treatment protocol. Conversely, solid mass development in CD4-deficient mice was significantly delayed with ASC/DMBQ therapy as compared to the responses of the corresponding controls ($p \leq 0.01$). The appearance of solid masses in CD8-deficient

Table I. Kinetics of T-Lymphocyte Depletion and Repopulation in BALB/c Mice[a]

Day	CD4+ T-Lymphocytes		CD8+ T-Lymphocytes	
	% Depletion	CD4:CD8	% Depletion	CD4:CD8
3	99.3 ± 0.02	0.01 ± 0.001	99.1 ± 0.3	95.2 ± 26.54
6	99.3 ± 0.2	0.02 ± 0.004	98.9 ± 0.1	71.0 ± 1.01
10	99.1 ± 0.1	0.02 ± 0.002	98.0 ± 0.1	41.8 ± 4.48
15	99.1 ± 0.1	0.01 ± 0.002	95.8 ± 0.3	18.0 ± 1.72
22	98.6 ± 0.2	0.03 ± 0.004	91.5 ± 0.6	16.1 ± 0.22
29	91.6 ± 1.9	0.19 ± 0.045	93.1 ± 0.1	11.3 ± 1.01

[a] Randomized mice were administered single ip injections of clarified hybridoma ascitic fluid (GK1.5 to deplete CD4+ T-lymphocytes and 2.43 to deplete CD8+ T-lymphocytes), as described in *Materials and Methods.* Cell suspensions were prepared from peripheral and mesenteric lymph nodes harvested from euthanized mAb-treated mice (n = 3 mice/treatment group) on the indicated time schedule, labelled for indirect immunofluorescence, and analyzed by flow cytometry. Results are expressed as mean % Depletion ± SEM and mean CD4:CD8 ratio ± SEM of triplicate values for the indicated assays.

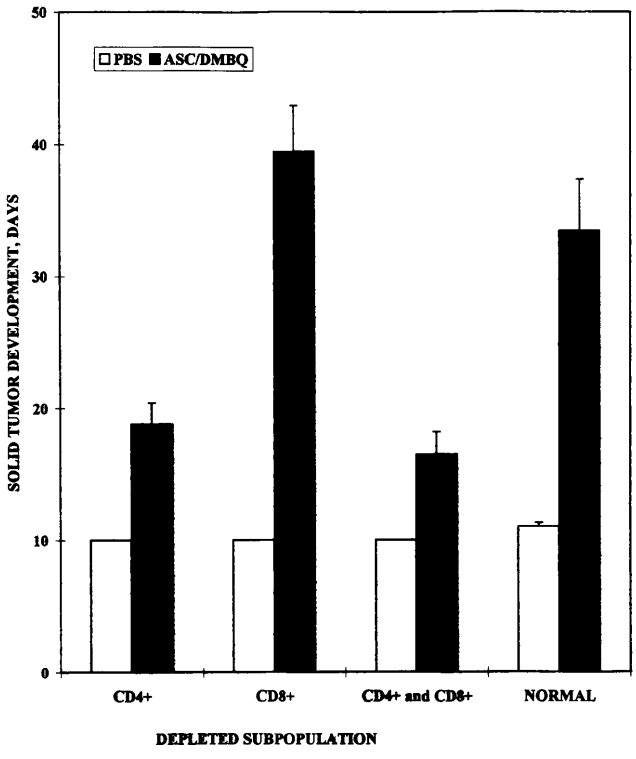

Figure 1. Solid tumor development in response to therapy and cellular deficiency. T-lymphocyte subpopulations were eliminated in randomized groups of mice (n = 10), challenged with tumor, and administered either ASC/DMBQ or PBS at two ip injections per day for seven consecutive days. This progressive manifestation of tumor growth provided an additional qualitative parameter to assess therapy-related tumor suppression. It is deemed consequential to the initial tumor implant and intradermal injury during subsequent multiple therapy injections. Results are expressed as the mean time of tumor development, in days, ± SEM.

ASC/DMBQ-treated mice was delayed for a considerably longer time frame over controls ($p \leq 0.01$), as well. Notably, maximal suppression of mass development was clearly evident in CD8-deficient mice following ASC/DMBQ therapy. Mice devoid of both subpopulations also responded with delayed tumor growth, but development times were substantially shorter than those of mice with either cellular deficiency. Normal immunocompetent mice developed solid masses at rates comparable to the responses of mice depleted of CD8+ cells.

The survival profiles of these groups of mice are shown in Table II. At 120 days post tumor implantation, the majority of CD8-deficient, ASC/DMBQ-treated mice survived. The mean survival time of this group was much longer than that of the concurrent PBS control group ($p \leq 0.002$). CD4-deficient mice survived longer with ASC/DMBQ therapy than the control mice ($p \leq 0.001$), but with a single long-term survivor at 120 days. ASC/DMBQ therapy did not enhance the mean survival time of mice devoid of both T-lymphocyte subpopulations when compared to the PBS control group ($p \geq 0.05$). However, ASC/DMBQ therapy did extend the mean survival time of normal, immunocompetent mice as opposed to the response of the normal control group ($p \leq 0.05$). Long-term survivors were not evaluated further for the acquired ability to reject secondary tumor challenge or to demonstrate altered leukocytic tumoricidal/tumoristatic properties.

Tumor Challenge Following ASC/DMBQ Therapy in Deficient Mice. Groups of randomized mice were depleted of T-lymphocyte subpopulations and administered the ASC/DMBQ therapy or PBS for 7 consecutive days. Tumor implantation was then performed in all mice 24 hr after the conclusion of the respective treatments. Tumor progression was then monitored daily, and survival profiles were determined through 22 days post tumor challenge, as shown in Figure 2. It can be seen that all normal immunocompetent mice and all CD8-deficient mice survived to this point after receiving ASC/DMBQ therapy. In contrast, with the exception of one mouse within the normal PBS control group, there were no other survivors in any other group, irrespective of treatment. These data demonstrated striking differences in treatment effect, which were dependent on specific deficiencies in T-lymphocyte subpopulations. These results suggest that CD4+ T-lymphocytes are critical to maximize the suppressive activity of ASC/DMBQ therapy.

The overall survival profiles of these mice are presented in Table III. The mean survival times of mice devoid of CD8+ cells (enriched for CD4+ cells) and normal immunocompetent mice were much greater than mice within the remaining experimental groups that received ASC/DMBQ therapy prior to tumor challenge. These two experimental groups were the only groups to demonstrate statistically significant effects when compared to the parallel PBS controls ($p \leq 0.001$ and $p \leq 0.05$, respectively). Therefore, these results suggest a definite correlation or synergism between the dimethoxybenzosemiquinone radical and functional CD4+ T-lymphocytes in suppressing tumor growth.

Impact of ASC/DMBQ Therapy on T-Lymphocyte Profiles Within Secondary Lymphoid Organs. T-lymphocyte subpopulation profiles of the spleen and pooled lymph node cell suspensions prepared from tumor-free control and ASC/DMBQ-treated mice are shown in Panels A and B of Figure 3. Minor fluctuations in CD4+ and CD8+ T-lymphocyte concentrations in spleen cell suspensions were observed over the indicated time course of 10 days, as shown in Panel A, but were not significantly different ($p \geq 0.05$) from the corresponding control suspensions. A marginal net increase in the CD8+ subpopulation was detected 3 days after conclusion of ASC/DMBQ therapy and suggests a possible delay in the mobilization of these lymphocytes. Similarly, the profiles of T-lymphocyte subpopulations in pooled lymph node cell suspensions from ASC/DMBQ-treated mice were not different from control profiles ($p \geq 0.05$), as shown in Panel B. Collectively, these results indicate that the standard 7-day ASC/DMBQ therapy has no definable negative impact on the distribution or viability of T-lymphocytes within the secondary lymphoid organs of tumor-free mice. T-lymphocytes from ASC/

Table II. Effect of T-Lymphocyte Deficiencies and ASC/DMBQ Therapy on Survival Profiles of Tumor-Bearing Mice

Deficiency[a]	Therapy[b]	Survival Profiles[c]				
		Range	Median	Mean ± SEM	p^d	Survivors
CD4	ASC/DMBQ	21–120	45.5	52.5 ± 9.1	≤0.01	1/10
	PBS	19–24	23	22.4 ± 0.5		0/10
CD8	ASC/DMBQ	27–120	120	85.1 ± 14.3	≤0.002	6/10
	PBS	23–45	24.5	26.5 ± 2.1		0/10
CD4 and CD8	ASC/DMBQ	2–54	33	28.5 ± 5.1	≥0.05	0/10
	PBS	19–24	23	22.3 ± 0.5		0/10
Normal	ASC/DMBQ	21–120	48	68.2 ± 14.4	≤0.05	4/10
	PBS	21–120	24.5	37.1 ± 9.9		1/10

[a] Randomized groups of mice (n = 10) were depleted of the indicated T-lymphocyte subpopulations, as previously described; Normal, immunocompetent mice with no induced cellular deficiencies.
[b] Therapies consisted of the indicated reagents at two ip injections per day for seven consecutive days administered to tumor-bearing mice with induced cellular deficiencies.
[c] Results are presented as survival profiles, in days, following ip tumor challenge, with mean survival times as the primary response data. Median survival times, ranges of survival, and numbers of survivors are included for additional comparisons. The study was terminated at 120 days post tumor challenge; mice that survived to this termination date were considered to have survival times of 120 days.
[d] Significance levels are from comparisons of mean survival times between ASC/DMBQ-treated mice and PBS control mice with the indicated cellular deficiencies.

DMBQ-treated mice responded to mitogenic stimulation with levels of thymidine incorporation comparable to concurrent PBS control suspensions (data not shown), suggesting no direct functional impairment.

Discussion

The reported effectiveness of ASC/DMBQ therapy against murine Ehrlich ascites tumor (7–9) provided insights into the potential antitumor effect(s) of long-lived semiquinone free radicals. Indeed, the free radicals exhibiting the longer half-lives, as measured by electron spin resonance, were also the more effective antitumor agents. The most dramatic results were obtained with a mixture of 750 mM ASC and 3 mM DMBQ, a naturally occurring quinone compound found in wheat germ (7). This combination of reagents was employed in these studies to retain protocol specificity. The Ehrlich ascites tumor used in these studies has been adapted for ip growth in the BALB/c mouse and is rapidly lethal to normal immunocompetent hosts without therapeutic intervention.

The inhibition of membrane-bound oxidases, as previously hypothesized (9), could not satisfactorily explain the high specificity for tumor cells that these reagents display *in vivo*. No evidence has been presented that the target enzymes are present in tumor cells only, and are absent in normal cells. We suspected, therefore, that other factors may have to account for this degree of specificity. In preliminary experiments reported earlier (22), we demonstrated that the efficacy of ASC/DMBQ therapy was dramatically compromised in immunodeficient mice. Indeed, little or no suppressive activity was documented in mice subjected to sublethal ionizing irradiation or to cyclosporin A therapy prior to tumor challenge. Suppressive activity was also absent in athymic nude mice, whereas tumor inhibition similar to that reported by Pethig *et al.* (7) was observed with normal immunocompetent mice.

The goals of the present studies were to evaluate the potential association of the semiquinone radical generated by ASC/DMBQ therapy with innate cell-mediated activities and to identify specific cell(s) capable of synergistic interaction to suppress tumor progression. The experimental approach involved modulating lymphocyte profiles *in vivo* and evaluating the subsequent effectiveness of this therapy in modifying tumor progression in test animals with these induced cellular deficiencies. The animal modeling proved adequate for assessing the impact of narrowly defined T-lymphocyte deficiencies on the cytostatic potential of ASC/DMBQ therapy. The manipulation of T-lymphocyte subpopulations in tumor-bearing mice altered the cytostatic potential of the therapy, and the semiquinone radical by association. These data, together with the results reported earlier (22), suggest that CD4+ T-lymphocytes and the dimethoxybenzosemiquinone free radical generated by this reagent combination cooperatively induce tumor suppression in Ehrlich ascites-bearing mice.

Semiquinone free radicals are capable of redox cycling in the presence of molecular oxygen, thereby generating the superoxide anion and regenerating the parent quinone. The production of reactive superoxide anions through semiquinone-quinone redox cycling may induce target cell damage

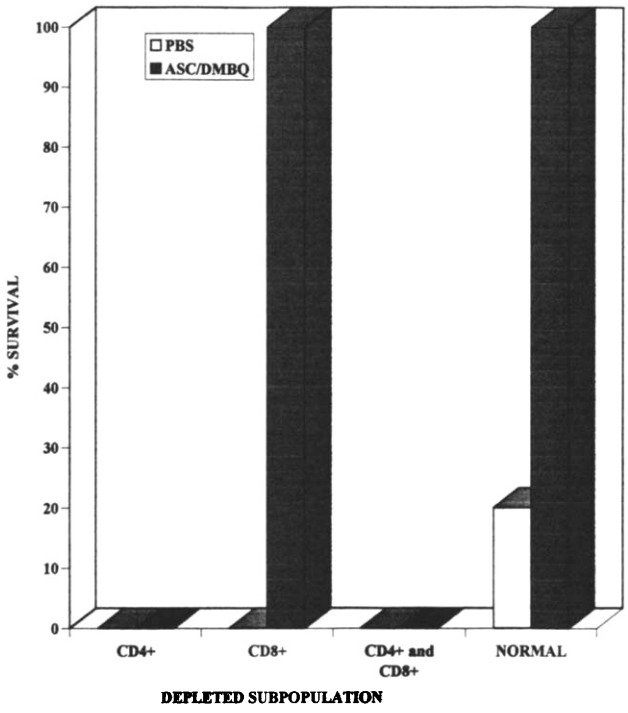

Figure 2. Survival profiles of immunodeficient mice challenged with tumor following therapy. T-lymphocyte subpopulations were eliminated in randomized groups of mice (n = 5), administered either ASC/DMBQ or PBS at two ip injections per day for seven consecutive days, then challenged with tumor. Results are shown as percentage of survival over time with an experimental time frame of 22 days post tumor challenge.

via indiscriminant intracellular reactions, including DNA degradation and protein damage (5, 6, 23, 24). However, it is difficult to visualize how such a mechanism or random attack could account for tumor cell specificity in host animals since oxygen-centered free radicals have notoriously short half-lives. Certain semiquinone radicals possess measured half-lives on the order of several minutes (7). The fact that we observed ASC/DMBQ-promoted suppressive activity in mice when tumor cells were implanted after the animals received the standard 7-day therapy suggests that reactive intermediates with much longer half-lives were involved. This observation, in fact, suggests that the semiquinone radical, rather than attacking the tumor cells directly, or indirectly *via* the formation of other short-lived radicals, may generate intermediates that are quite stable with varied activities, including elucidating responses of certain cells involved in cellular immunity.

It should be noted that a variety of chemotherapeutic agents, including several quinone and quinone-like compounds such as benzoquinone, adriamycin, and mitomycin C, have been shown to interact with various immune response cells (25–27), resulting in enhanced immunocytotoxic functions (28–33). Thus, peritoneal macrophages, mast cells, natural killer cells, and cytotoxic T-lymphocytes have been subjected to various *in vitro* manipulations to characterize the mode-of-action of several quinone-based therapeutic agents. Nonquinone anticancer agents have also been evaluated for immunological interactions within the context of therapeutic effect(s), such as BCNU (34), BEPH (35), cisplatin (36–38), and synthetic flavonoid compounds (20, 39, 40).

The results of the present studies demonstrate the necessity for functional CD4+ T-lymphocytes to optimize the suppressive effect of this semiquinone free radical toward Ehrlich ascites tumor cells. These data further confirm the transient nature of the observed cytostatic effect of this free radical against this particular tumor model. Therefore, it is

Table III. Comparison of Survival Profiles of Immunocompetent and T-Lymphocyte Deficient Mice Administered Therapies Prior to Tumor Challenge[a]

Deficiency	Therapy	Survival Profiles[b]			
		Range	Median	Mean ± SEM	p[c]
CD4	ASC/DMBQ	17–2	19	18.6 ± 0.5	≥0.05
	PBS	15–20	19	18.4 ± 0.9	
CD8	ASC/DMBQ	23–29	28	26.8 ± 1.1	≤0.001
	PBS	17–23	10	19.2 ± 1.0	
CD4 and CD8	ASC/DMBQ	13–19	17	16.4 ± 1.3	≥0.05
	PBS	15–19	19	17.8 ± 0.8	
Normal	ASC/DMBQ	25–32	25	27.8 ± 1.7	≤0.05
	PBS	19–29	21	22.4 ± 1.9	

[a] Randomized groups of mice (n = 5) were depleted of the indicated T-lymphocyte subpopulations, as previously described; Normal, immunocompetent mice with no induced cellular deficiencies. Therapies consisted of the indicated reagents at two ip injections per day for seven consecutive days, then challenged with lethal tumor load by ip injection 24 hr later.
[b] Results are presented as survival profiles, in days, following tumor challenge, with mean survival times as the primary response data.
[c] Significant differences in mean survival times between ASC/DMBQ-treated and PBS control mice were observed only in groups with functional CD4+ T-lymphocytes (*via* mAb-induced elimination of CD8+ T-lymphocytes) and with normal immunocompetent mice.

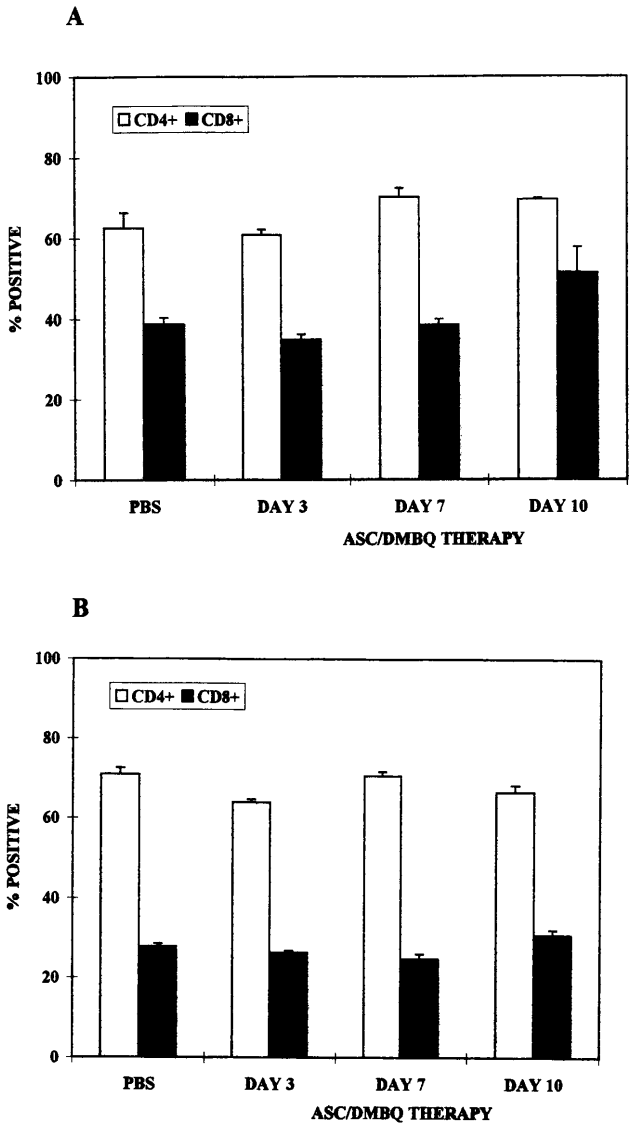

Figure 3. Effect of ASC/DMBQ therapy on T-lymphocyte profiles in secondary lymphoid organs of tumor-free mice. Randomized tumor-free mice were administered the seven-day ASC/DMBQ therapy. Single cell suspensions were prepared from spleens (Panel A) and pooled lymph nodes (Panel B), then stained for cellular identification by indirect immunofluorescence and flow cytometry, as previously described. Results are expressed as mean percent positive ± SEM for CD4+ and CD8+ T-lymphocytes (n = 3 per indicated day with ASC/DMBQ therapy and n = 6 for PBS controls).

postulated that therapy-induced cytostatis and T-lymphocyte participation act synergistically to retard rapid tumor progression in this particular system. However, these observations were made with one chemotherapeutic agent, using one tumor model in a single animal species. Since in-bred BALB/c mice were employed in these studies, rather than out-bred CD1 mice referenced by Pethig *et al.* (7), and different variants of the Ehrlich ascites tumor were employed in the respective investigations, it could be argued that the original protocol continuity was compromised. However, it is our contention that the efficacy of ASC/DMBQ therapy has been convincingly confirmed in a different animal model challenged with a fast growing, rapidly lethal ip tumor. Manipulating the cellular immune system of the recipient mice provided strong evidence of CD4+ T-lymphocyte participation in the suppressive effect of ASC/DMBQ therapy, and by inference, the dimethoxybenzosemiquinone free radical generated by this reagent combination.

1. Brunmark A, Cadenas E. Redox and addition chemistry of quinoid compounds and its biological implications. Free Rad Biol Med **7:**435–477, 1989.
2. Powis G. Metabolism and reactions of quinoid anticancer agents. Pharmacol Ther **35:**57–162, 1987.
3. Gutierrez PL. Mechanism(s) of bioreductive activation: The example of diaziquinone (AZQ). Free Rad Biol Med **6:**405–445, 1989.
4. Bachur NR, Gordon SL, Gee MV. A general mechanism for microsomal activation of quinone anticancer agents to free radicals. Cancer Res **38:**1745–1750, 1978.
5. Halliwell B, Gutteridge JM. Oxygen toxicity, oxygen radicals, transition metals, and disease. Biochem J **219:**1–14, 1984.
6. Keizer HG, Pinedo HM, Schuurhuis GJ, Joenje H. Doxorubicin (adriamycin): A critical review of free radical-dependent mechanisms of cytotoxicity. Pharmacol Ther **47:**219–231, 1990.
7. Pethig R, Gascoyne PRC, McLaughlin JA, Szent-Gyorgyi A. Ascorbate-quinone interactions: Electrochemical, free radical, and cytotoxic properties. Proc Natl Acad Sci USA **80:**129–132, 1983.
8. Pethig R, Gascoyne PRC, McLaughlin JA, Szent-Gyorgyi A. Interaction of the 2,6-dimethoxysemiquinone and ascorbyl free radicals with Ehrlich ascites cells: A probe of surface cell charge. Proc Natl Acad Sci USA **81:**2088–2091, 1984.
9. Pethig R, Gascoyne PRC, McLaughlin JA, Szent-Gyorgyi A. Enzyme-controlled scavenging of ascorbyl and 2,6-dimethoxysemiquinone free radicals in Ehrlich ascites tumor cells. Proc Natl Acad Sci USA **82:**1439–1442, 1985.
10. Byrnes RW, Templin J, Sem D, Lyman S, Petering DH. Intracellular DNA strand scission and growth inhibition of Ehrlich ascites tumor cells by bleomycins. Cancer Res **50:**5275–5286, 1990.
11. Fecchio D, Russo M, Sirois P, Braquet P, Jancar S. Inhibition of Ehrlich ascites tumor *in vivo* by PAF-antagonists. Int J Immunopharmacol **12:**57–65, 1990.
12. Friche E, Jensen PB, Roed H, Skovsgaard T, Nissen NI. *In vitro* circumvention of anthracycline-resistance in Ehrlich ascites tumor by anthracycline analogues. Biochem Pharmacol **39:**1721–1726, 1990.
13. Friche E, Danks MK, Schmidt CA, Beck WT. Decreased DNA topoisomerase II in daunorubicin-resistant Ehrlich ascites tumor cells. Cancer Res **51:**4213–4218, 1991.
14. Sprent J, Schaffer M. Properties of purified T cell subsets. I. *In vitro* responses to class I vs. class II H-2 alloantigens. J Exp Med **162:**2068–2088, 1985.
15. Hornbeck P. Enzyme-linked immunosorbent assays. In: Coligan JE, Kruisbeek AM, Margulies DH, Shevach EM, Stober W, Eds. Current Protocols in Immunology. New York: John Wiley & Sons, Vol 1:p 2.1.2, 1991.
16. Morrow KJ, Unuvar E, King SW, Mleczko JB. Techniques for the production of monoclonal and polyclonal antibodies. In: Hayat MA, Ed. Colloidal Gold: Principles, Methods, and Applications. San Diego: Academic Press, Inc., Vol 3:p 31, 1991.
17. Husmann LA, Bevan MJ. Cooperation between helper T cells and cytotoxic T lymphocyte precursors. In: Battisto JR, Plate J, Shearer G, Eds. Cytotoxic T Cells: Biology and Relevance to Disease. New York: The New York Academy of Sciences, Vol 532:p 158, 1988.
18. Chou T, Shu S. Cellular interactions and the role of interleukin 2 in the expression and induction of immunity against a syngeneic murine sarcoma. J Immunol **139:**2103–2109, 1987.
19. Gorozny J, Weyand CM, Fathman CG. Long-term humoral unresponsiveness *in vivo* induced by treatment with monoclonal antibody against L3T4. J Exp Med **164:**911–925, 1986.

20. Pratesi G, Rodolfo M, Rovetta G, Parmiani G. Role of T cells and tumor necrosis factor in antitumor activity and toxicity of flavone acetic acid. Eur J Cancer **26:**1079–1083, 1990.
21. Sasaki DT, Dumas SE, Engleman EG. Discrimination of viable and non-viable cells using propidium iodide in two-color immunofluorescence. Cytometry **8:**413–420, 1987.
22. Morgan CD, Combs SH, Everse J. Probable immune system mediation of the antitumor activity of the 2,6-dimethoxybenzo-p-semiquinone radical. Proc Soc Exp Biol Med **208:**294–299, 1994.
23. Cummings J, Anderson L, Willmott N, Smyth JF. The molecular pharmacology of doxorubicin *in vivo*. Eur J Cancer **27:**532–535, 1991.
24. Doroshow JH, Akman S, Chu F-F, Esworth S. Role of the glutathione-glutathione peroxidase cycle in the cytotoxicity of the anticancer quinones. Pharmacol Ther **47:**359–370, 1990.
25. Afanas'ev IB, Korkina LG, Suslova TB, Soodaeva SK. Are quinones producers or scavengers of superoxide ion in cells? Arch Biochem Biophys **281:**245–250, 1990.
26. Ogura T, Shindo H, Namba M, Yamamura Y. Tumoricidal activity of peritoneal exudate cells from rats treated with mitomycin C. Jpn J Cancer Res **71:**920–921, 1980.
27. Stoychkov JN, Schultz RM, Chirigos MA, Pavlidis NA, Goldin A. Effects of adriamycin and cyclophosphamide treatment on induction of macrophage cytotoxic function in mice. Cancer Res **39:**3014–3017, 1979.
28. Bourguet-Kondracki M-I, Longeon A, Morel E, Guyot M. Sesquiterpene quinones as immunomodulating agents. Int J Immunopharmacol **13:**393–399, 1991.
29. Ehrke MJ, Ryoyama K, Cohen S. Cellular basis for adriamycin-induced augmentation of cell-mediated cytotoxicity in culture. Cancer Res **44:**2497–2504, 1984.
30. Ehrke MJ, Maccubin D, Ryoyama K, Cohen SA, Mihich E. Correlation between adriamycin-induced augmentation of interleukin 2 production and cell-mediated cytotoxicity in mice. Cancer Res **46:**54–60, 1986.
31. Haskill JS. Adriamycin-activated macrophages as tumor growth inhibitors. Cancer Res **41:**3852–3856, 1981.
32. Martin FA, Caignard A, Olsson O, Jeannin JF, Leclerc A. Tumoricidal effect of macrophages exposed to adriamycin *in vivo* or *in vitro*. Cancer Res **42:**3851–3857, 1982.
33. Santoni A, Riccardi A, Sorci V, Herberman RB. Effects of adriamycin on the activity of mouse natural killer cells. J Immunol **1224:**2329–2335, 1980.
34. Sensi M, Bergomi M, Formelli F, Parmiani G. Eradication of a disseminated mouse lymphoma by 1,3-bis(2-chloroethyl)-1-nitrosurea is immunologically mediated and accompanied by *de novo* generation of anti-tumor cytotoxicity. Int J Cancer **46:**1088–1094, 1990.
35. Bowlin TL, Prakash NJ, Edwards ML, Sjoerdsma A. Participation of T-lymphocytes in the curative effect of a novel synthetic polyamine analogue, N′-bis[3-(ethylamino)propyl]-1, 7-heptanediamine, against L1210 leukemia *in vivo*. Cancer Res **51:**62–66, 1991.
36. Sodhi A, Singh SM. Increased capacity of lymphocytes to lyse tumor cells *in vitro* and production of lymphotoxins after cisplatin treatment. Int J Immunopharmacol **10:**753–761, 1988.
37. Sodhi A, Pai K, Singh RK, Singh SM. Activation of human NK cells and monocytes with cisplatin *in vitro*. Int J Immunopharmacol **12:**893–898, 1990.
38. Sodhi A, Singh RK, Pai K. Activation of murine macrophages by tumor necrosis factor, interleukin-1, interferon-gamma and cisplatin. Immunol Lett **26:**45–50, 1990.
39. Bibby MC, Phillips RM, Double JA, Pratesi G. Anti-tumor activity of flavone acetic acid (NSC 347512) in mice-influence of immune status. Br J Cancer **63:**57–62, 1991.
40. Damia G, Tagliabue G, Allavena P, D'Incalci M. Flavone acetic acid antitumor activity against a mouse pancreatic adenocarcinoma is mediated by natural killer cells. Cancer Immunol Immunother **32:**241–244, 1990.